Editors' Suggestion

Spin Subdiffusion in the Disordered Hubbard Chain

Maciej Kozarzewski,[1] Peter Prelovšek,[2,3] and Marcin Mierzejewski[4]
[1]Institute of Physics, University of Silesia, 40-007 Katowice, Poland
[2]J. Stefan Institute, SI-1000 Ljubljana, Slovenia
[3]Faculty of Mathematics and Physics, University of Ljubljana, SI-1000 Ljubljana, Slovenia
[4]Department of Theoretical Physics, Faculty of Fundamental Problems of Technology, Wrocław University of Science and Technology, 50-370 Wrocław, Poland

(Received 26 March 2018; published 13 June 2018)

We derive and study an effective spin model that explains the anomalous spin dynamics in the one-dimensional Hubbard model with strong potential disorder. Assuming that charges are localized, we show that spins are delocalized and their subdiffusive transport originates from a singular random distribution of spin exchange interactions. The exponent relevant for the subdiffusion is determined by the Anderson localization length and the density of the electrons. Although the analytical derivations are valid for low particle density, numerical results for the full model reveal a qualitative agreement up to half filling.

DOI: 10.1103/PhysRevLett.120.246602

Introduction.—The many-body localization (MBL) [1,2] has recently been intensively studied. A vast amount of numerical data allowed us to identify the main properties of MBL systems: vanishing steady transport, [3–10] absence of thermalization [11–31], and logarithmic growth of entanglement entropy [15,17,32–35]. It has also been found that MBL prevents a driven system from heating up [9,36–41]. These unusual properties can be explained via the existence of a macroscopic number of local integrals of motion [12,25,26,42–47].

While most theoretical studies so far concentrated on the one-dimensional (1D) disordered model of interacting spinless fermions, experiments on MBL are performed on cold-fermion lattices [14,48–50] in which the relevant model is the Hubbard model with spin-1/2 fermions, whereby the disorder enters only via a random (or quasiperiodic) charge potential. Recent numerical studies of such a model [47,51–53] reveal that even at strong disorder, localization and nonergodicity occur only in the charge subsystem, implying a partial MBL. Unless one also introduces an additional random magnetic field [47,54], the spin remains delocalized [52,55–59] although the spin transport is anomalously slow and subdiffusive [52].

In this Letter, we focus on an explanation of the slow spin dynamics and subdiffusion within the disordered 1D Hubbard model. We first demonstrate that in the case of potential disorder and low particle density the spin dynamics can be described by a squeezed isotropic Heisenberg model, whereby the distribution of the random exchange interactions is singular. Such an effective model can be studied numerically quite in detail, but also analytically by taking into account that the 1D spin dynamics is dominated by weak links. In this manner, we show that spin excitations spread over distance M in a characteristic time t such that $M \propto t^{\alpha}$ with $\alpha \simeq \lambda/(d+\lambda)$, where d is the average distance between singly occupied sites and λ is determined by the Anderson localization length in the noninteracting system. Although the mapping on the Heisenberg model is valid for dilute systems $d \gg 1$, numerical results for strongly disordered Hubbard model reveal that the same qualitative spin dynamics remains valid for all densities even up to half filling.

Model.—Our aim is to establish the spin dynamics in the disordered Hubbard chain,

$$H = -t_h \sum_{i\sigma} (c^{\dagger}_{i+1\sigma} c_{i\sigma} + \text{H.c.}) + \sum_i \varepsilon_i n_i + U \sum_i n_{i\uparrow} n_{i\downarrow}, \quad (1)$$

where $n_i = n_{i\uparrow} + n_{i\downarrow}$ and $n_{i\sigma} = c^{\dagger}_{i\sigma} c_{i\sigma}$. We study the model with L sites and N electrons, fixing also the total spin projection $S^z_{\text{tot}} = 0$. We assume a uniform distribution of random charge potentials, $\varepsilon_i \in [-W, W]$, and we set the hopping integral $t_h = 1$.

Two electrons.—In order to gain a preliminary insight to the spin dynamics, we first study two electrons. The dynamics of a few interacting spinless particles has been studied previously [60–62]. Here, we study for illustration $N = 2$ electrons with opposite spin projections that propagate on the chain with $L = 16$ sites. Assuming that particles are initially at sites j and l, $|\psi(0)\rangle = c^{\dagger}_{l\downarrow} c^{\dagger}_{j\uparrow} |0\rangle$, the propagation of $|\psi(t)\rangle$ is obtained via exact diagonalization. Figures 1(a) and 1(b) show, respectively, the time dependence of the local spin $\langle S^z_i \rangle(t) = \frac{1}{2} \langle \psi(t) | n_{i\uparrow} - n_{i\downarrow} | \psi(t) \rangle$ and the density $\langle n_i \rangle(t) = \langle \psi(t) | n_i | \psi(t) \rangle$ for one configuration of ε_i corresponding to $W = 8$. Although for such strong disorder the charge degrees appear to be fully localized, spins undergo oscillations.

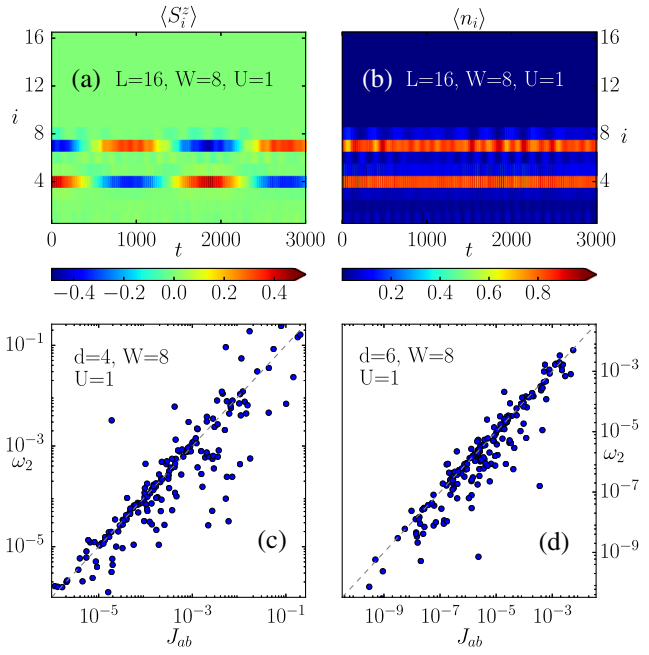

FIG. 1. Two electrons on the disordered Hubbard chain. (a), (b) $\langle S_i^z\rangle(t)$ and $\langle n_i\rangle(t)$ for a single initial state and single realization of disorder. (c),(d) Frequency ω_2 of spin oscillation obtained directly from the Hubbard model [see panel (a)] compared with Eq. (4). The distance between electrons is fixed at $d = 4$ (c) and $d = 6$ (d).

Effective spin model.—The coexistence of almost frozen charges and oscillating spins suggests that one can derive an effective spin model, e.g., see Refs. [63,64]. To this end, we use the Anderson states as the basis; i.e., we use the single-particle eigenstates, $\phi_{ia} = \langle i|a\rangle$, of the noninteracting ($U = 0$) model. Then,

$$H = \sum_{a\sigma} \epsilon_a c^\dagger_{a\sigma} c_{a\sigma} + \frac{U}{2} \sum_{aa'bb'\sigma} \chi^{ab}_{a'b'} c^\dagger_{a\sigma} c^\dagger_{b\bar{\sigma}} c_{b'\bar{\sigma}} c_{a'\sigma},$$
$$\chi^{ab}_{a'b'} = \sum_i \phi^*_{ia}\phi^*_{ib}\phi_{ib'}\phi_{ia'}. \tag{2}$$

Assuming that the charge dynamics is frozen, the main effect arising from the presence of the Coulomb interaction comes from terms with either $a = a'$, $b = b'$ or $a = b'$, $b = a'$. Then, the Hubbard term in Eq. (2) can be written in a SU(2)-invariant form

$$H_U = \frac{1}{2}\sum_{a\neq b} J_{ab}\left(\frac{1}{4} n_a n_b - \vec{S}_a \cdot \vec{S}_b\right), \tag{3}$$

where we use standard density and spin operators: $n_a = n_{a\uparrow} + n_{a\downarrow}$, $S^z_a = \frac{1}{2}(n_{a\uparrow} - n_{a\downarrow})$, $S^+_a = c^\dagger_{a\uparrow} c_{a\downarrow}$, $S^-_a = c^\dagger_{a\downarrow} c_{a\uparrow}$. The effective exchange interaction is ferromagnetic

$$J_{ab} = 2U\chi^{ab}_{ab} = 2U\sum_i |\phi_{ia}|^2 |\phi_{ib}|^2. \tag{4}$$

In Eq. (3) we have omitted the term $U\sum_a \chi^{aa}_{aa} n_{a\uparrow} n_{a\downarrow}$. Since there is no direct hopping between the Anderson states, $n_{a\uparrow} n_{a\downarrow}$ remains frozen.

In order to test the approximate equation (4), we consider $N = 2$ electrons with opposite spins, located at sites j and $j + d$. We evaluate the spin-oscillation frequency, ω_2, directly from results for the Hubbard model; see Fig. 1(a). For the same set of ϵ_i, we then identify Anderson states a, b that maximize $|\phi_{ja}|^2$ and $|\phi_{j+db}|^2$, respectively. This enables the calculation of J_{ab} from Eq. (4) that should lead to spin oscillations $\langle S^z_{j,l}\rangle = \pm\frac{1}{2}\cos(J_{ab}t)$. Figures 1(c) and 1(d) show correlations between ω_2 and J_{ab} for various realizations of disorder and various distances d between the electrons. One finds that indeed $\omega_2 \simeq J_{ab}$ for strong disorder $W \gg 1$ and $d \gg 1$.

For a low density of carriers and a larger disorder, the maxima of the occupied Anderson states a and b are typically separated by $x_{ab} > \xi$, exceeding the single-particle localization length, ξ. Then, one obtains an approximate relation

$$J_{ab} \simeq 2U\exp(-x_{ab}/\lambda), \qquad \lambda \sim \xi. \tag{5}$$

The squeezed spin model.—Assuming that charges are frozen to the initial occupations $n_i = 0$, 1, 2, it is evident that the effective spin model (3) acts only on singly occupied sites with $n_i = 1$. The spin dynamics of the Hubbard model at high temperatures $T \gg W$, U can be then studied by first randomly positioning N electrons on L sites. This allows us to establish the distribution of distances between the singly occupied sites as well as the distribution of the effective J_{ab}, using Eq. (4) or its simplified version, Eq. (5). Because of the exponential decay of J_{ab}, we consider only couplings between the neighboring singly occupied sites. The effective Heisenberg model on a squeezed chain then reads

$$H_H = -\sum_i J_i \vec{S}_i \cdot \vec{S}_{i+1}, \tag{6}$$

where the summation is carried out over singly occupied sites $n_i = 1, i \in \{1, \ldots, \tilde{N}\}$ with $\tilde{N} \leq N$. Note that at infinite temperature, the average lattice spacing in the effective model equals $d = L/\tilde{N} = (\bar{n} - \bar{n}^2/2)^{-1}$, where $\bar{n} = N/L$ is the average filling in the original Hubbard model.

In order to establish the probability distribution of J_i, we first consider a section of length $L \gg 1$, where we randomly choose the continuous positions of $\tilde{N} = L/d$ points. The probability density for the distances between the neighboring points is $f_d(x) = (1/d)\exp(-x/d)$. Although the latter result has formally been obtained for continuous positions of points, it should hold true also for discrete positions of singly occupied sites provided that $d \gg 1$. Using this result, one may find the probability density for the random exchange interaction $f_J(J)$. To this

end, we use Eq. (5) and compare the cumulative distribution functions

$$\int_0^y dx \frac{1}{d}\exp\left(-\frac{x}{d}\right) = \int_{2U\exp(-y/\lambda)}^{2U} dJ f_J(J). \quad (7)$$

Taking the derivative of Eq. (7) with respect to y and introducing the dimensionless interaction $\tilde{J} = J/2U$, one gets

$$f_{\tilde{J}}(\tilde{J}) = \tilde{\lambda}\tilde{J}^{\tilde{\lambda}-1}, \qquad \tilde{\lambda} = \lambda/d. \quad (8)$$

Since the latter distribution was derived from Eq. (5), it holds for $\lambda/d \ll 1$. It is clear that the interaction U sets the energy scale (and the time scale) of the effective model, whereas the qualitative spin dynamics depends on the ratio between the effective localization length λ and the interparticle distance d. The important message is that for low doping ($d \gg 1$) and strong disorder ($\lambda \sim 1$) one obtains $\tilde{\lambda} \ll 1$ with the distribution of $\tilde{J}$ being singular at $\tilde{J} = 0$. Still, $\lim_{\delta\to 0^+} \int_0^\delta d\tilde{J} f_{\tilde{J}}(\tilde{J}) = 0$; hence the probability for cutting the Heisenberg chain into disconnected subchains is vanishingly small. Note that singularity in Eq. (8) is integrable for $\tilde{\lambda} > 0$.

In order to test the accuracy of Eq. (8), we have also numerically generated the distribution of $\tilde{J} = J_{ab}/2U$ directly from Eq. (4), in the same way as discussed for the $N = 2$ case. The positions of the two electrons l and j have been randomly chosen in such a way that the distance $x = |l - j|$ is distributed according to $f_d(x)$ for various d. The numerical results for $W = 4$ and 8 are shown in Figs. 2(a) and 2(b), respectively. These results have been fitted by Eq. (8), whereby we adjusted a single parameter λ for all values of d. We have obtained $\lambda \simeq 0.75$ and $\lambda \simeq 0.4$ for $W = 4$ and $W = 8$, respectively. Although Eq. (8) has been derived for $d \gg 1$, it turns out to remain qualitatively valid also for $d = 2$, i.e., for the average distance between singly occupied sites in the half-filled Hubbard model. We conclude that Eq. (8) accurately describes $f_{\tilde{J}}(\tilde{J})$ at least for small $\tilde{J}$, i.e., in the regime that is essential for the long-time spin dynamics.

Local spin correlations.—We first calculate the time-dependent local spin correlations at infinite temperature,

$$S_L(t) = \langle S_i^z S_i^z(t)\rangle = \frac{1}{\mathrm{Tr}\,1}\langle \mathrm{Tr}[S_i^z(t) S_i^z]\rangle_{\mathrm{dis}}, \quad (9)$$

where the spin evolution is determined by the effective H_H. We take the random interaction $J_i = \tilde{J}$ as given by Eq. (8); i.e., we express time in units of $1/2U$. The term $\langle\ldots\rangle_{\mathrm{dis}}$ means averaging over various realizations of J_i, and we use at least 2000 disorder samples.

Figures 2(c) and 2(d) show $S_L(t)$. For longer times and $\tilde{\lambda} < 1$, one observes power-law decay $S_L(t) \propto (2Ut)^{-\alpha}$ with $\alpha < 1/2$; hence, the spin dynamics is clearly subdiffusive. In Fig. 3(a) we demonstrate α obtained from fitting numerical results by $S_L(t) \propto t^{-\alpha}$ in the time window $t \in [10, 50]$. The main message coming from these studies is that $\alpha > 0$ for arbitrary nonzero $\tilde{\lambda} > 0$, i.e., for arbitrary nonzero filling. For $\tilde{\lambda} \ll 1$ we obtain the exponent $\alpha \simeq \tilde{\lambda}$. Still, it should be noted that the distribution (8) is singular only for $\tilde{\lambda} < 1$, which should be the regime of subdiffusion. For $\tilde{\lambda} \ll 1$ the finite size effects are negligible [Fig. 2(c)] but become significant for larger $\tilde{\lambda}$, Fig. 2(d). Nevertheless, for the regime with $\tilde{\lambda} \simeq 1$ (relevant for larger filling $\bar{n} \sim 1$ and/or weaker disorder), our results shown in Fig. 2(d) are consistent with normal spin diffusion with $\alpha = 1/2$, which is also expected in the weakly disordered Hubbard model. Results in Figs. 2(c), 2(d), and 3(a) support the scenario that the spin excitations spread subdiffusively due to the singular distribution of random exchange interactions, Eq. (8).

Single weak-link scenario.—To explain the relation of the subdiffusive dynamics and the singular distribution of $\tilde{J}_i$, we consider a single spin excitation and estimate the time t in which the excitation spreads over M sites in the effective Heisenberg chain. We assume the weak-link scenario, in which the long time dynamics is governed by rare regions with the smallest J_i. A similar approach has been used to describe the subdiffusive transport of spinless

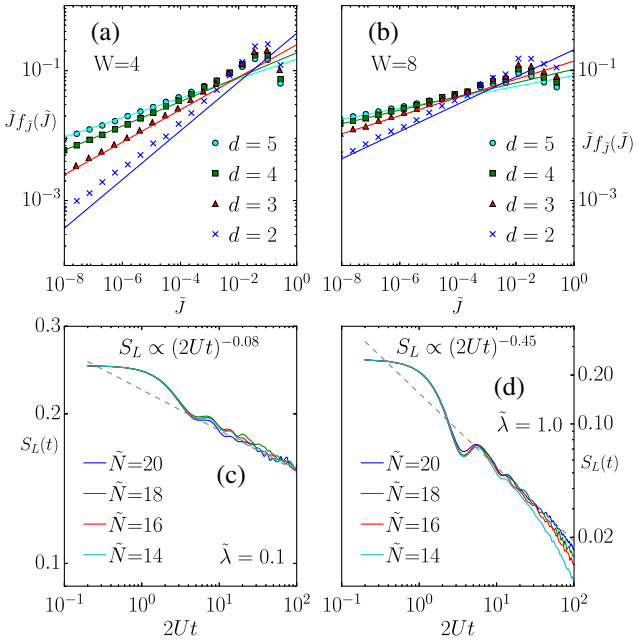

FIG. 2. Points in (a),(b) show $\tilde{J}f_{\tilde{J}}(\tilde{J})$, generated directly from Eq. (4) for $N = 2$ electrons at the average distance d, whereby results have been fitted to Eq. (8) by adjusting a single λ (for all d). (c),(d) Local spin correlation function [Eq. (9)] for the effective model with various numbers of spins $\tilde{N}$. The results for $t \in [10, 50]$ with the largest $\tilde{N}$ are fitted by $S_L(t) \propto t^{-\alpha}$ shown as the dashed line.

particles in the vicinity of the MBL transition [5,50,65,66] or in quasiperiodic potential [67]. Here, we assume that $t \sim 1/(2U\tilde{J}_m)$, where $\tilde{J}_m$ is the weakest exchange out of $\tilde{J}_i$ for $i = 1, \ldots, M$. The probability that each random $\tilde{J}_i$ is larger than $\tilde{J}_0$ is

$$\left(\int_{\tilde{J}_0}^{1} d\tilde{J} f_{\tilde{J}}(\tilde{J})\right)^M = \int_{\tilde{J}_0}^{1} d\tilde{J}_m f_m(\tilde{J}_m), \qquad (10)$$

where $f_m(\tilde{J}_m)$ is the probability density for the smallest interaction. Using Eq. (8) and calculating the derivative of Eq. (10) with respect to $\tilde{J}_0$, one finds the distribution function $f_m(\tilde{J}_0) = \tilde{\lambda} M \tilde{J}_0^{\tilde{\lambda}-1}(1-\tilde{J}_0^{\tilde{\lambda}})^{M-1}$. Then, the expectation value of the smallest exchange interaction out of M random $\tilde{J}_i$ reads

$$\langle \tilde{J}_m \rangle = \int_0^1 d\tilde{J}_m f_m(\tilde{J}_m)\tilde{J}_m \simeq \Gamma\left(1+\frac{1}{\tilde{\lambda}}\right) M^{-1/\tilde{\lambda}}, \qquad (11)$$

where we have used formulas for asymptotics at $M \gg 1/\tilde{\lambda}$. So we find the relation between the spread of the spin excitations Λ and t as

$$\Lambda \sim Md \propto (2Ut)^{\tilde{\lambda}}, \qquad S_L(t) \propto M^{-1} \propto (2Ut)^{-\tilde{\lambda}}. \qquad (12)$$

The exponent $\alpha = \tilde{\lambda}$ is the same as that previously obtained from numerical studies of the effective Heisenberg model for $\tilde{\lambda} \ll 1$.

Multiple weak-link scenario.—The simple single-weak link scenario breaks down for $\tilde{\lambda} \sim 1$, where $\alpha \simeq \tilde{\lambda}/2$ instead of $\tilde{\lambda}$, as shown in Fig. 2(d). As a more general explanation for the subdiffusive transport, we consider distribution of effective *hopping times* between neighboring sites in the squeezed spin model. The relevant dimensionless quantity is $\tau = 1/\tilde{J}$. Using Eq. (8), one finds the probability density $f_\tau(\tau) = \tilde{\lambda}/\tau^{\tilde{\lambda}+1}$. For such a broad distribution of hopping times in a *classical* model of random traps [68,69], one gets subdiffusive transport $\Lambda \propto (2Ut)^{\alpha}$ where $\alpha = \tilde{\lambda}/(1+\tilde{\lambda})$ for $\tilde{\lambda} < 1$. In the latter model, a classical particle may hop between neighboring traps in time τ. The hopping time τ is randomly chosen for each site, but it remains the same for each visit of the same site. This simple model quite accurately reproduces the dynamical exponent α for arbitrary $\tilde{\lambda}$, as shown in Fig. 3(a), whereas for $\tilde{\lambda} \ll 1$ it gives the same relation as the single weak-link scenario. For $\tilde{\lambda} \ll 1$, the transport (in both scenarios) is governed by the weakest links. However, in order to describe the entire subdiffusive regime, one should go beyond the single weak-link picture and also account for other links.

Comparison with the Hubbard model.—Finally, we compare our analytical predictions with numerical results obtained directly for the Hubbard model. The time-dependent local spin correlation function $S_L(t)$ at infinite temperature has been obtained using the microcanonical Lanczos method (MCLM) [70,71] (in analogy to the *imbalance* correlations presented previously [52]) for the Hubbard model with $L = 18$ and $N = 6$; i.e., $d \simeq 3.5$. The results are shown in Figs. 3(b) and 3(c) together with the analytical prediction, $S_L(t) \propto (2Ut)^{-\alpha}$ with $\alpha = \lambda/(\lambda+d)$ and λ obtained from fits in Fig. 2(b). Despite significant finite size effects, one observes that the latter estimate correctly describes the subdiffusive spin dynamics in the Hubbard model at low filling $\bar{n} \ll 1$. In particular, exponent α obtained directly from the Hubbard model weakly depends on U.

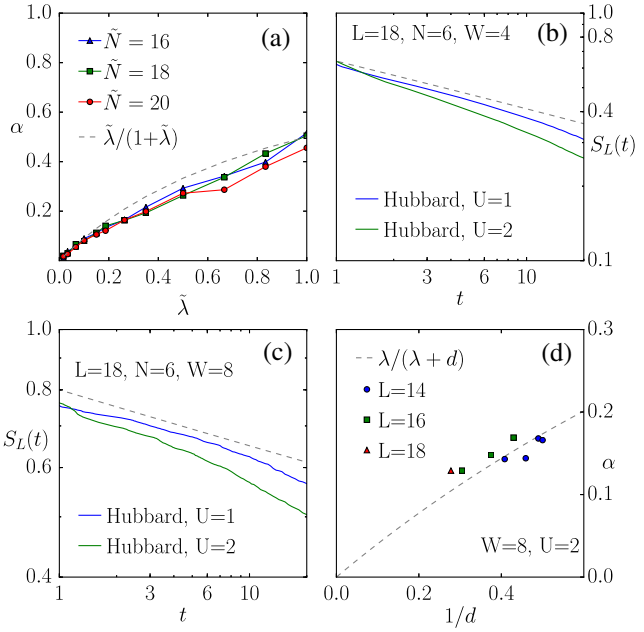

FIG. 3. (a) Dynamical exponent α vs $\tilde{\lambda}$ obtained for the squeezed model. (b),(c) Spin-spin correlation function obtained for the Hubbard model ($L = 18$, $N = 6$) and compared with $t^{-\alpha}$ (dashed line), where $\alpha = \lambda/(\lambda+d)$. (d) α in the Hubbard model ($U = 2$, $W = 8$, various N and L). λ in (b)–(d) is obtained from fits in Fig. 2(b).

Moreover, one can consider the validity of the subdiffusion scenario in the full Hubbard model beyond the limit of low filling. It has previously been found that spins reveal a subdiffusive dynamics even for $\bar{n} = 1$ [52]. We therefore analyze the MCLM results for $S_L(t) \propto t^{-\alpha}$ considering various system sizes $L = 14$, 16, 18 and various numbers of electrons N. For the time window $t \in [1, 10]$, we extract the dynamical exponent α and compare with $\alpha = \lambda/(\lambda+d)$, as shown in Fig. 3(d). Our approach works even up to $\bar{n} = 1$ since the average distance between singly occupied sites $d \geq 2$, while $\lambda < 1$ provided that the disorder is sufficiently strong. In particular, for $W = 8$ and $\bar{n} \leq 1$, we have estimated that $\tilde{\lambda} \lesssim 0.2$.

Conclusions.—In this Letter, we presented an explanation for the anomalous spin dynamics in a 1D Hubbard model with large potential disorder in the regime of partial

MBL, where the charge dynamics appears to be frozen whereas spins exhibit ergodic but subdiffusive transport [52]. We have derived an effective isotropic Heisenberg model with random exchange interactions between neighboring singly occupied sites J_i. Our derivation is formally best applicable to the regime of low filling, $\bar{n} \ll 1$, and strong disorder. The main origin of the subdiffusive behavior then appears to be the singular distribution of the effective exchange interaction J_i with the crucial parameter $\tilde{\lambda} = \lambda/d$ representing the ratio of the single-particle Anderson localization length and the average distance between singly occupied sites. Results for the Hubbard model reveal that such a scenario seems to remain qualitatively valid beyond the considered limits of low filling, even at $\bar{n} = 1$, provided that the disorder is sufficiently strong. It appears that there is no threshold filling $\bar{n}_c$, below which spins would also become localized and full MBL would prevail.

There are still questions concerning the dynamics within the disordered Hubbard model, also being relevant to cold-atom experiments on MBL [14,48–50]. Our derivation of the effective model remains on the level of spin dynamics, while charge degrees are assumed to be frozen. It is evident that higher order terms in the Anderson basis, following from Eq. (2), would also lead to the dynamical coupling between charge and spin degrees of freedom. Since the spin dynamics is ergodic, it is not excluded that charges would also eventually delocalize, but then on much larger time scales.

This Letter is supported by the National Science Centre, Poland, via project 2016/23/B/ST3/00647 (M. M. and M. K.), and P. P. acknowledges the support of program P1-0044 of the Slovenian Research Agency.

[1] D. M. Basko, I. L. Aleiner, and B. L. Altshuler, Metal-insulator transition in a weakly interacting many-electron system with localized single-particle states, Ann. Phys. (Amsterdam) **321**, 1126 (2006).
[2] V. Oganesyan and D. A. Huse, Localization of interacting fermions at high temperature, Phys. Rev. B **75**, 155111 (2007).
[3] T. C. Berkelbach and D. R. Reichman, Conductivity of disordered quantum lattice models at infinite temperature: Many-body localization, Phys. Rev. B **81**, 224429 (2010).
[4] O. S. Barišić and P. Prelovšek, Conductivity in a disordered one-dimensional system of interacting fermions, Phys. Rev. B **82**, 161106 (2010).
[5] K. Agarwal, S. Gopalakrishnan, M. Knap, M. Müller, and E. Demler, Anomalous Diffusion and Griffiths Effects Near the Many-body Localization Transition, Phys. Rev. Lett. **114**, 160401 (2015).
[6] Y. Bar Lev, G. Cohen, and D. R. Reichman, Absence of Diffusion in an Interacting System of Spinless Fermions on a One-dimensional Disordered Lattice, Phys. Rev. Lett. **114**, 100601 (2015).
[7] R. Steinigeweg, J. Herbrych, F. Pollmann, and W. Brenig, Scaling of the optical conductivity in the transition from thermal to many-body localized phases, Phys. Rev. B **94**, 180401(R) (2016).
[8] O. S. Barišić, J. Kokalj, I. Balog, and P. Prelovšek, Dynamical conductivity and its fluctuations along the crossover to many-body localization, Phys. Rev. B **94**, 045126 (2016).
[9] M. Kozarzewski, P. Prelovšek, and M. Mierzejewski, Distinctive response of many-body localized systems to a strong electric field, Phys. Rev. B **93**, 235151 (2016).
[10] P. Prelovšek and J. Herbrych, Self-consistent approach to many-body localization and subdiffusion, Phys. Rev. B **96**, 035130 (2017).
[11] A. Pal and D. A. Huse, Many-body localization phase transition, Phys. Rev. B **82**, 174411 (2010).
[12] M. Serbyn, Z. Papić, and D. A. Abanin, Local Conservation Laws and the Structure of the Many-body Localized States, Phys. Rev. Lett. **111**, 127201 (2013).
[13] Y. Bar Lev and D. R. Reichman, Dynamics of many-body localization, Phys. Rev. B **89**, 220201 (2014).
[14] M. Schreiber, S. S. Hodgman, P. Bordia, H. P. Lüschen, M. H. Fischer, R. Vosk, E. Altman, U. Schneider, and I. Bloch, Observation of many-body localization of interacting fermions in a quasi-random optical lattice, Science **349**, 842 (2015).
[15] M. Serbyn, Z. Papić, and D. A. Abanin, Criterion for Many-body Localization-Delocalization Phase Transition, Phys. Rev. X **5**, 041047 (2015).
[16] V. Khemani, R. Nandkishore, and S. L. Sondhi, Nonlocal adiabatic response of a localized system to local manipulations, Nat. Phys. **11**, 560 (2015).
[17] D. J. Luitz, N. Laflorencie, and F. Alet, Extended slow dynamical regime prefiguring the many-body localization transition, Phys. Rev. B **93**, 060201 (2016).
[18] I. V. Gornyi, A. D. Mirlin, and D. G. Polyakov, Interacting Electrons in Disordered Wires: Anderson Localization and Low-t Transport, Phys. Rev. Lett. **95**, 206603 (2005).
[19] E. Altman and R. Vosk, Universal dynamics and renormalization in many-body-localized systems, Annu. Rev. Condens. Matter Phys. **6**, 383 (2015).
[20] A. De Luca and A. Scardicchio, Ergodicity breaking in a model showing many-body localization, Europhys. Lett. **101**, 37003 (2013).
[21] C. Gramsch and M. Rigol, Quenches in a quasidisordered integrable lattice system: Dynamics and statistical description of observables after relaxation, Phys. Rev. A **86**, 053615 (2012).
[22] A. De Luca, B. L. Altshuler, V. E. Kravtsov, and A. Scardicchio, Anderson Localization on the Bethe Lattice: Nonergodicity of Extended States, Phys. Rev. Lett. **113**, 046806 (2014).
[23] D. A. Huse, R. Nandkishore, V. Oganesyan, A. Pal, and S. L. Sondhi, Localization-protected quantum order, Phys. Rev. B **88**, 014206 (2013).
[24] R. Nandkishore and D. A. Huse, Many-body-localization and thermalization in quantum statistical mechanics, Annu. Rev. Condens. Matter Phys. **6**, 15 (2015).
[25] L. Rademaker and M. Ortuño, Explicit Local Integrals of Motion for the Many-Body Localized State, Phys. Rev. Lett. **116**, 010404 (2016).

[26] A. Chandran, I. H. Kim, G. Vidal, and D. A. Abanin, Constructing local integrals of motion in the many-body localized phase, Phys. Rev. B **91**, 085425 (2015).
[27] V. Ros, M. Müller, and A. Scardicchio, Integrals of motion in the many-body localized phase, Nucl. Phys. **B891**, 420 (2015).
[28] J. Eisert, M. Friesdorf, and C. Gogolin, Quantum many-body systems out of equilibrium, Nat. Phys. **11**, 124 (2015).
[29] M. Serbyn, M. Knap, S. Gopalakrishnan, Z. Papić, N. Y. Yao, C. R. Laumann, D. A. Abanin, M. D. Lukin, and E. A. Demler, Interferometric Probes of Many-Body Localization, Phys. Rev. Lett. **113**, 147204 (2014).
[30] P. Sierant, D. Delande, and J. Zakrzewski, Many-body localization due to random interactions, Phys. Rev. A **95**, 021601 (2017).
[31] P. Prelovšek, O. S. Barišić, and M. Mierzejewski, Reduced-basis approach to many-body localization, Phys. Rev. B **97**, 035104 (2018).
[32] M. Žnidarič, T. Prosen, and P. Prelovšek, Many-body localization in the Heisenberg *XXZ* magnet in a random field, Phys. Rev. B **77**, 064426 (2008).
[33] J. H. Bardarson, F. Pollmann, and J. E. Moore, Unbounded Growth of Entanglement in Models of Many-Body Localization, Phys. Rev. Lett. **109**, 017202 (2012).
[34] J. A. Kjäll, J. H. Bardarson, and F. Pollmann, Many-body Localization in a Disordered Quantum Ising Chain, Phys. Rev. Lett. **113**, 107204 (2014).
[35] M. Serbyn, Z. Papić, and D. A. Abanin, Universal Slow Growth of Entanglement in Interacting Strongly Disordered Systems, Phys. Rev. Lett. **110**, 260601 (2013).
[36] D. A. Abanin, W. De Roeck, W. W. Ho, and F. Huveneers, Effective Hamiltonians, prethermalization, and slow energy absorption in periodically driven many-body systems, Phys. Rev. B **95**, 014112 (2017).
[37] D. A. Abanin, W. De Roeck, and F. Huveneers, Exponentially Slow Heating in Periodically Driven Many-body Systems, Phys. Rev. Lett. **115**, 256803 (2015).
[38] P. Ponte, Z. Papić, F. Huveneers, and D. A. Abanin, Many-body Localization in Periodically Driven Systems, Phys. Rev. Lett. **114**, 140401 (2015).
[39] P. Bordia, H. Lüschen, U. Schneider, M. Knap, and I. Bloch, Periodically driving a many-body localized quantum system, Nat. Phys. **13**, 460 (2017).
[40] S. Choi, J. Choi, R. Landig, G. Kucsko, H. Zhou, J. Isoya, F. Jelezko, S. Onoda, H. Sumiya, V. Khemani, C. von Keyserlingk, N. Y. Yao, E. Demler, and M. D. Lukin, Observation of discrete time-crystalline order in a disordered dipolar many-body system, Nature (London) **543**, 221 (2017).
[41] J. Zhang, P. W. Hess, A. Kyprianidis, P. Becker, A. Lee, J. Smith, G. Pagano, I.-D. Potirniche, A. C. Potter, A. Vishwanath, N. Y. Yao, and C. Monroe, Observation of a discrete time crystal, Nature (London) **543**, 217 (2017).
[42] D. A. Huse, R. Nandkishore, and V. Oganesyan, Phenomenology of fully many-body-localized systems, Phys. Rev. B **90**, 174202 (2014).
[43] J. Z. Imbrie, V. Ros, and A. Scardicchio, Local integrals of motion in many-body localized systems, Ann. Phys. (Berlin) **529**, 1600278 (2017).
[44] T. E. O'Brien, D. A. Abanin, G. Vidal, and Z. Papić, Explicit construction of local conserved operators in disordered many-body systems, Phys. Rev. B **94**, 144208 (2016).
[45] S. Inglis and L. Pollet, Accessing Many-body Localized States through the Generalized Gibbs Ensemble, Phys. Rev. Lett. **117**, 120402 (2016).
[46] M. Goihl, M. Gluza, C. Krumnow, and J. Eisert, Construction of exact constants of motion and effective models for many-body localized systems, Phys. Rev. B **97**, 134202 (2018).
[47] M. Mierzejewski, M. Kozarzewski, and P. Prelovšek, Counting local integrals of motion in disordered spinless-fermion and Hubbard chains, Phys. Rev. B **97**, 064204 (2018).
[48] J.-Y. Choi, S. Hild, J. Zeiher, P. Schauß, A. Rubio-Abadal, T. Yefsah, V. Khemani, D. A. Huse, I. Bloch, and C. Gross, Exploring the many-body localization transition in two dimensions, Science **352**, 1547 (2016).
[49] P. Bordia, H. P. Lüschen, S. S. Hodgman, M. Schreiber, I. Bloch, and U. Schneider, Coupling Identical 1D Many-body Localized Systems, Phys. Rev. Lett. **116**, 140401 (2016).
[50] P. Bordia, H. Lüschen, S. Scherg, S. Gopalakrishnan, M. Knap, U. Schneider, and I. Bloch, Probing Slow Relaxation and Many-body Localization in Two-dimensional Quasiperiodic Systems, Phys. Rev. X **7**, 041047 (2017).
[51] R. Mondaini and M. Rigol, Many-body localization and thermalization in disordered Hubbard chains, Phys. Rev. A **92**, 041601(R) (2015).
[52] P. Prelovšek, O. S. Barišić, and M. Žnidarič, Absence of full many-body localization in the disordered Hubbard chain, Phys. Rev. B **94**, 241104 (2016).
[53] J Bonča and M. Mierzejewski, Delocalized carriers in the t-J model with strong charge disorder, Phys. Rev. B **95**, 214201 (2017).
[54] G. Lemut, M. Mierzejewski, and J. Bonča, Complete Many-Body Localization in the t-J Model Caused by a Random Magnetic Field, Phys. Rev. Lett. **119**, 246601 (2017).
[55] A. C. Potter and R. Vasseur, Symmetry constraints on many-body localization, Phys. Rev. B **94**, 224206 (2016).
[56] A. Chandran, V. Khemani, C. R. Laumann, and S. L. Sondhi, Many-body localization and symmetry-protected topological order, Phys. Rev. B **89**, 144201 (2014).
[57] I. V. Protopopov, W. W. Ho, and D. A. Abanin, Effect of SU(2) symmetry on many-body localization and thermalization, Phys. Rev. B **96**, 041122 (2017).
[58] A. J. Friedman, R. Vasseur, A. C. Potter, and S. A. Parameswaran, Localization-protected order in spin chains with non-Abelian discrete symmetries, arXiv:1706.00022.
[59] S. A. Parameswaran and S. Gopalakrishnan, Spin-catalyzed hopping conductivity in disordered strongly interacting quantum wires, Phys. Rev. B **95**, 024201 (2017).
[60] D. L. Shepelyansky, Coherent Propagation of Two Interacting Particles in a Random Potential, Phys. Rev. Lett. **73**, 2607 (1994).
[61] Ph. Jacquod and D. L. Shepelyansky, Two Interacting Quasiparticles above the Fermi Sea, Phys. Rev. Lett. **78**, 4986 (1997).
[62] D. Schmidtke, R. Steinigeweg, J. Herbrych, and J. Gemmer, Interaction-induced weakening of localization in few-particle disordered Heisenberg chains, Phys. Rev. B **95**, 134201 (2017).

[63] Y. B. Lev, D. R. Reichman, and Y. Sagi, Many-body localization in system with a completely delocalized single-particle spectrum, Phys. Rev. B **94**, 201116 (2016).

[64] C. W. Duncan, N. J. S. Loft, P. Öhberg, N. T. Zinner, and M. Valiente, Spin localization of a fermi polaron in a quasirandom optical lattice, Few-Body Syst. **58**, 50 (2017).

[65] K. Agarwal, E. Altman, E. Demler, S. Gopalakrishnan, D. A. Huse, and M. Knap, Rare region effects and dynamics near the many body localization transition, Ann. Phys. (Berlin) **529**, 1600326 (2017).

[66] H. P. Lüschen, P. Bordia, S. Scherg, F. Alet, E. Altman, U. Schneider, and I. Bloch, Observation of Slow Dynamics near the Many-Body Localization Transition in One-Dimensional Quasiperiodic Systems, Phys. Rev. Lett. **119**, 260401 (2017).

[67] Y. Bar Lev, D. M. Kennes, C. Klöckner, D. R. Reichman, and C. Karrasch, Transport in quasiperiodic interacting systems: From superdiffusion to subdiffusion, Europhys. Lett. **119**, 37003 (2017).

[68] J.-P. Bouchaud and A. Georges, Anomalous diffusion in disordered media: Statistical mechanisms, models and physical applications, Phys. Rep. **195**, 127 (1990).

[69] J. Machta, Random walks on site disordered lattices, J. Phys. A **18**, L531 (1985).

[70] M. W. Long, P. Prelovšek, S. El Shawish, J. Karadamoglou, and X. Zotos, Finite-temperature dynamical correlations using the microcanonical ensemble and the Lanczos algorithm, Phys. Rev. B **68**, 235106 (2003).

[71] P. Prelovšek and J. Bonča, in *Strongly Correlated Systems—Numerical Methods* (Springer, Berlin, 2013).